Eur. Phys. J. B **29**, 211–215 (2002)
DOI: 10.1140/epjb/e2002-00288-4

THE EUROPEAN PHYSICAL JOURNAL B

Self-affine random surfaces

O.I. Yordanov[1,2,a] and I.S. Atanasov[2]

[1] American University in Bulgaria, 2700 Blagoevgrad, Bulgaria
[2] Institute of Electronics, BAS, 1784 Sofia, Bulgaria

Received 3 October 2001 / Received in final form 5 March 2002
Published online 2 October 2002 –

Abstract. We consider general d-dimensional random surfaces that are characterized by power-law power spectra defined in both infinite and finite spectral regions. The first type of surfaces belongs to the class of ideal fractals, whereas the second possess both the smallest and the largest scales and physically is more realistic. For both types we calculate the structure functions (SF) exactly; in addition for the second type we obtain the SF's asymptotic expansions. On this basis we show that the surfaces are (in statistical sense) self-affine and approximately self-affine, respectively. Depending on the value of the spectral exponent, we find imbalance between the finite size effects which results in systematic discrepancy in the scaling properties between the two types of surfaces. Explicit expressions for the topothesy, and in the case of second type of surfaces for the large correlation length and cross-over distances are also derived.

PACS. 02.50.Ey Stochastic processes – 68.35.Bs Surface structure and topography – 68.35.Ct Interface structure and roughness

1 Introduction

We study two classes of self-affine d-dimensional isotropic random surfaces, embedded in $\mathbb{R}^{d+1}$. Both types of surfaces, considered as realizations of a random field, $f(\boldsymbol{x})$, $\boldsymbol{x} \in \mathbb{R}^d$ are constructed on basis of their spectral representation, assuming power-law spectral density. The study generalizes results obtained earlier for the case $d = 1$, see [1,2]. The first type of surfaces, considered in the next section, is characterized by power-law spectra, $S(k) = Ak^{-\alpha}$ extending over all positive wave-numbers k. The values of the spectral exponent α are assumed to be restricted within $d < \alpha < d+2$. In this case the surface has infinite variance and autocovariance function. We calculate the structure function (SF) of the surface, which is finite and shows that the surface is exactly (in statistical sense) self-affine. This case is referred to as ideal fractal surfaces in $\mathbb{R}^{d+1}$. The Hausdorff (fractal) dimension D of these surfaces is related solely to the spectral exponent α.

The second class of surfaces which we consider in Section 3 below is represented by a stochastic field defined by finite domain power-law spectra with two absolutely sharp cutoffs. Moments of arbitrary order exist for these fields. We calculate the pertaining SF in terms of type (1, 2) hypergeometric function and obtain its asymptotic expansions. On this basis we identify three intervals of $|\boldsymbol{x}|$ values within which the SF behavior is qualitatively different. For small $|\boldsymbol{x}|$, the SF is to a leading order quadratic, whereas for large arguments it follows an oscillatory behavior. The most interesting properties of the surfaces are inferred from the asymptotic at intermediate $|\boldsymbol{x}|$. The dominant term follows power-law functional form, systematically distorted, however by the lower order terms. The latter are associated with the effects due to the finite size of the system. Further, there exists an imbalance between the finite size effects: the effect of the largest scale (related to the lowest cutoff) is more pronounced when α is close to $d+2$, while the effect of the smallest scale/highest cutoff occurs at $\alpha \gtrsim d$. This analysis justifies the definition of the second class of surfaces as being approximately self-affine.

In the last section we summarize the obtained results and enlist some the applications. A useful representation and the asymptotic expansion of the ${}_1F_2$ hypergeometric function are given in the Appendix.

2 Ideal fractal surfaces

It is convenient to define the fields of interest, as Fourier-Stielties integrals (spectral representation [3])

$$f(\boldsymbol{x}) = \int \exp(\mathrm{i}\boldsymbol{k}\cdot\boldsymbol{x})\,\mathrm{d}z(\boldsymbol{k}), \tag{1}$$

where $\boldsymbol{x}$ and $\boldsymbol{k}$ are d-dimensional vectors and z is a random field with zero mean and orthogonal increments. More specifically, $\langle z(\boldsymbol{k})\rangle = 0$ and

$$\langle \mathrm{d}z^*(\boldsymbol{k})\,\mathrm{d}z(\boldsymbol{k'})\rangle = \delta(\boldsymbol{k}-\boldsymbol{k'})S(\boldsymbol{k})\mathrm{d}\boldsymbol{k}\mathrm{d}\boldsymbol{k'}. \tag{2}$$

(We use broken brackets to denote the ensemble average.) In (2) $S(\boldsymbol{k})$ is called spectral density function, which if

[a] e-mail: oyordanov@aubg.bg

specified, defines (1) throughout moments of second order and if f is a Gaussian field, completely. We should note that (1) represents a surface without self intersection and overhanging. A typical physical example in which the random field (1) serves as a model is provided by the heights of a rough surface above a reference plane, $h = f(\boldsymbol{x})$, where $\boldsymbol{x} \in \mathbb{R}^2$. Using (1) and (2), it is easy to obtain an integral representation (involving $S(\boldsymbol{k})$) for the main object of our considerations, namely, the structure function associated with the field f

$$\Delta_{(f)}(\boldsymbol{x}) = \left\langle [f(\boldsymbol{x}_0 + \boldsymbol{x}) - f(\boldsymbol{x}_0)]^2 \right\rangle; \tag{3}$$

also referred as mean square increments function [4]. It is related to the autocovariance function of f, defined by $\mathcal{A}_{(f)}(\boldsymbol{x}) = \langle f(\boldsymbol{x}_0 + \boldsymbol{x}) f(\boldsymbol{x}_0) \rangle$ through $\Delta_{(f)}(\boldsymbol{x}) = 2\sigma^2 - 2\mathcal{A}_{(f)}(\boldsymbol{x})$, where σ^2 denotes the variance of the surface. For isotropic fields $S(\boldsymbol{k})$ depends on the magnitude of $\boldsymbol{k}$ only $S = S(k)$, $k = |\boldsymbol{k}|$: respectively $\Delta_{(f)}$ is a function of $x = |\boldsymbol{x}|$. Changing to spherical coordinates and taking $d-1$ angular integrations (3) is brought to the following convenient form:

$$\Delta_{(f)}(x) = \frac{4\pi^{d/2}}{\Gamma(d/2)} \times \int_0^\infty \left[1 - {}_0F_1\left(\frac{d}{2}; -\frac{k^2x^2}{4}\right)\right] S(k) k^{d-1}\,\mathrm{d}k, \tag{4}$$

where ${}_0F_1$ denotes type (0, 1) hypergeometric function. (${}_0F_1$ from these parameter and argument can be expressed in terms of order $(d/2-1)$ Bessel function [5].)

In the context of our study the ideal fractal surfaces are generated by specifying for every k in (2):

$$S(k) = Ak^{-\alpha}, \tag{5}$$

where A is a (spectral) constant and the values of the spectral exponent are restricted within $d < \alpha < d+2$. In order to show that $f(\boldsymbol{x})$ is exactly self-affine (in statistical sense) we calculate $\Delta_{(f)}$ explicitly. The restriction on the α values ensures the finiteness of the integral (4). Note that if considered separately, the terms in the integrand of (4) are divergent. Since these terms represent essentially the variance and the autocovariance function, the latter quantities do not exist for ideal fractal surfaces. Substituting (5), changing variables, $u = kx/2$, and performing integration by parts once we have

$$\Delta_{(f)}(x) = \frac{2A\pi^{d/2}x^{\alpha-d}}{(d-\alpha)\Gamma(d/2+1)} \times \int_0^\infty {}_0F_1\left(d/2+1; -u\right) u^{(d-\alpha)/2}\mathrm{d}u. \tag{6}$$

The integral in (6) represents the Melin transform from $\Gamma(d/2+1)\Gamma\left[(d+2-\alpha)/2\right]/\Gamma(\alpha/2)$. To see this, consider the inverse Melin transform from $G(s) = \Gamma(\mu)\Gamma(s)/\Gamma(\mu - s)$ and close the contour of integration by the left semi-circle at infinity. The residues of $G(s)$ at $0, -1, -2, \ldots$ exactly reproduce the terms of the ${}_0F_1\left(\mu; -u\right)$ expansion. Putting $s = (d+2-\alpha)/2$ and $\mu = d/2+1$ in $G(s)$ we recover the integral in (6). This evaluation is similar to the one used in the proof of the Slater theorem [6]. As a final result:

$$\Delta_{(f)}(x) = \tau^{d+2-\alpha} x^{\alpha-d}, \tag{7}$$

where:

$$\tau^{d+2-\alpha} = \frac{A\pi^{d/2}2^{d+2-\alpha}\Gamma\left((d+2-\alpha)/2\right)}{(\alpha-d)\Gamma(\alpha/2)}\,. \tag{8}$$

Expressions (7) and (8) for the cases $d = 1$ and $d = 2$, were first obtained in [4]. Equation (7) shows that $f(\boldsymbol{x})$ is exactly self-affine with scaling exponent $H = (\alpha - d)/2$; sometimes H is called the Hurst exponent. Its fractal (Hausdorff) dimension D is related to the spectral exponent α by $D = d + 1 - (\alpha - d)/2$, [7]. When f is used as a model of rough surfaces, τ is called topothesy [8,4]. If, in general, $f(\boldsymbol{x})$ has a physical dimension identical with x, then τ has the same dimension and equation (7) shows that over a 'distance' $x = \tau$, the mean increment of f is precisely τ. *I.e.* the small (fractality) scale fluctuations of f are determined by τ only. Clearly, (8) diverges in both $\alpha \to d$ and $\alpha \to d+2$ limits, see Figure 1, where τ is plotted as a function of H and for several spatial dimensions.

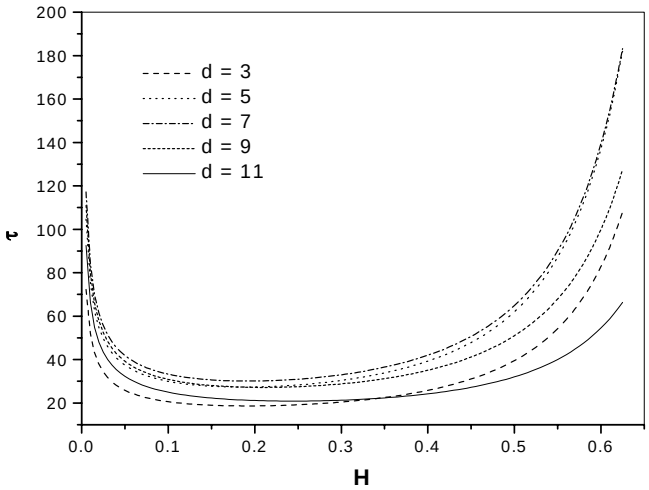

Fig. 1. Graphs of τ, see (8), *vs.* $H = (\alpha - d)/2$ for five different spatial dimensions d given in the legends.

3 Approximate self-affine surfaces

We turn now to the physically more realistic case of surfaces having power-law spectra defined over finite domain spectral interval with two absolutely sharp cut-offs:

$$S(k) = \begin{cases} Ak^{-\alpha}, & \text{if } k_0 \le k \le k_1 \\ 0, & \text{otherwise.} \end{cases}, \tag{9}$$

assuming again $d < \alpha < d+2$. Either by direct integration of (4) or by using the integral representation (22) in the Appendix, the structure function associated with (9) can be written in the form of

$$\Delta_{(f)}(x) = \Delta_0(x) - \Delta_1(x), \tag{10}$$

where $\Delta_p(x)$, $p = 0, 1$, are expressed in terms of type $(1, 2)$ hypergeometric function

$$\Delta_p(x) = 2\sigma_p^2 \left[1 - {}_1F_2 \left(\frac{d-\alpha}{2}; \frac{d+2-\alpha}{2}, \frac{d}{2}; -\frac{k_p^2 x^2}{4} \right) \right], \tag{11}$$

and

$$\sigma_p^2 = \frac{2A\pi^{d/2}}{\Gamma(d/2)} \frac{k_p^{d-\alpha}}{(\alpha - d)}, \qquad p = 0, 1. \tag{12}$$

It follows from (10–12) that the variance of the field is:

$$\sigma^2 = \frac{1}{2}\Delta_{(f)}(\infty) = \sigma_0^2 - \sigma_1^2. \tag{13}$$

Equation (10) incorporates the expressions for the case $d = 1$ obtained in [1]. It should be noted also that equations (10–13) in fact hold for all $\alpha > d$, provided $\alpha \neq d + 2n$, $n = 1, 2, \ldots$ It is important to stress that the first term in (10) involves only k_0, the parameter associated with the largest scale of the surface, whereas the second – k_1 the parameter associated with the smallest scale.

There are three intervals of x values within which the SF behaviour is qualitatively different. At small distances, $x \leq k_1^{-1}$, $\Delta_{(f)}$ increases to the leading approximation quadratically, refer to (10). To infer the behaviour of $\Delta_{(f)}$ for intermediate distances, roughly given by $k_1^{-1} \ll x < k_0^{-1}$, we substitute for Δ_1 its asymptotic expansion which follows from the asymptotic form of ${}_1F_2$, see equation (23) of the Appendix:

$$\Delta_{(f)}(x) = \tau^{d+2-\alpha} x^{\alpha-d} + \Delta_0(\alpha, x) - \Lambda_1(\alpha, x) \tag{14}$$

where the expression for τ is the same as that given by (8), and the notation

$$\Lambda_p(\alpha, x) = 2\sigma_p^2 \times \left[1 + \frac{(\alpha - d)}{d} {}_0F_1 \left(\frac{d+2}{2}; -\frac{k_p^2 x^2}{4} \right) Y_0(k_p x) - \frac{(\alpha - d)}{k_p x} {}_0F_1 \left(\frac{d}{2}; -\frac{k_p^2 x^2}{4} \right) Y_1(k_p x) \right], \tag{15}$$

$p = 0, 1$, with

$$Y_q(z) = \sum_{n=0}^{\infty} (-1)^n \left(\frac{\alpha}{2} \right)_{n+q} \left(\frac{\alpha - d}{2} + 1 \right)_n \left(\frac{2}{z} \right)^2, \tag{16}$$

is introduced. In Y_q, $q = 0$ or 1 and $(a)_b$ is the Pocchammer's notation [5].

The magnitudes of the second and the third terms related to the magnitude of the first term in (14), to the leading orders, are $(k_0 x)^{d+2-\alpha}$ and $(1/k_1 x)^{\alpha-d}$, respectively. Hence, the dominant asymptotic term of the SF follows a power-low behaviour, identical to the one exhibited in the case of ideal fractal surfaces, which shows that the random field associated with (9) is approximately self-affine. This symmetry, however, is distorted when α is close to $d + 2$ by the effect due to the largest spatial scale of the structure; alternatively, the smallest scale affects the SF mostly for α close to d. To see this, note that if α is close to d, $(k_0 x)^{d+2-\alpha} \approx 0$, but $(1/k_1 x)^{\alpha-d} \approx 1$. On the other hand, if $\alpha \lesssim d + 2$, $(k_0 x)^{d+2-\alpha} \approx 1$ and $(1/k_1 x)^{\alpha-d} \approx 0$. This imbalance of the two finite site effects leads to a systematic discrepancy between the scaling exponent (measured from the log-log plot of $\Delta_{(f)}(x)$) and the exponent expected on the basis of the ideal fractal analog: $2H = \alpha - d$. Similar discrepancy occurs if one attempts to infer α using some of the algorithms for fractal dimension estimation [9]. This effect for d-dimensional field is similar to the one-dimensional case discussed in detail in [1,2], see Figure 2, where the SFs, of both ideal fractal (dotted line) and finite-domain power-law spectra surfaces (solid line) are plotted in a ($\log_2$-$\log_2$) scale for $d = 4$, $\alpha = 4.1 \gtrsim d$ and $A = 0.01$. The values of the cut-off wave-numbers used to produce the solid line are given in the legends. It is seen that the dominance of the effect of the smallest spatial scale over the effect of the largest leads to a steeper slope of the SF compared to the slope of the ideal fractal surface SF.

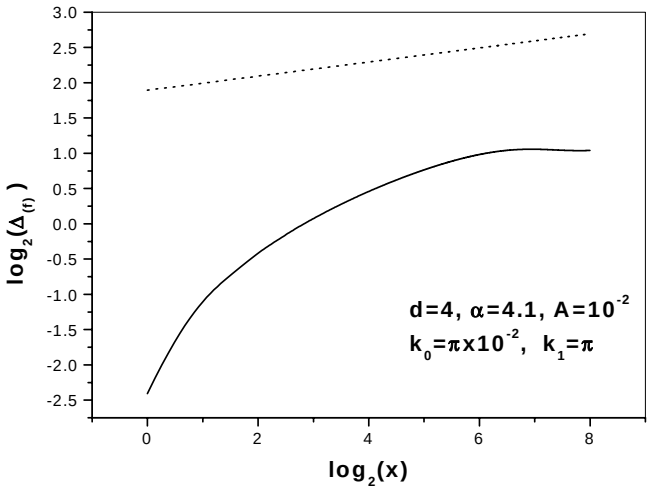

Fig. 2. Graphs of the structure functions for ideal fractal surface (dotted line) and for the surface with finite-domain power-law spectrum (solid line). The spectral parameters used to produce both graphs are given in the legends. Observe that due to the imbalance between the finite-size effects the slope of the solid line in the scaling interval is steeper than $2H = \alpha - d = 0.1$, the slope of the ideal fractal SF.

Just the opposite is seen in the case of $\alpha \lesssim d+2$. Now the effect of the largest size is prevailing and as a result, the slope of the SF, corresponding to the finite-domain spectra, is smaller compared to the ideal fractal SF, see Figure 3.

For even larger $x \gg k_0^{-1}$, we substitute the asymptotic form of $\Delta_0(x)$ in (14) to infer the second asymptotic regime of $\Delta_{(f)}(x)$

$$\Delta_{(f)}(x) \sim \Lambda_0(\alpha, x) - \Lambda_1(\alpha, x). \tag{17}$$

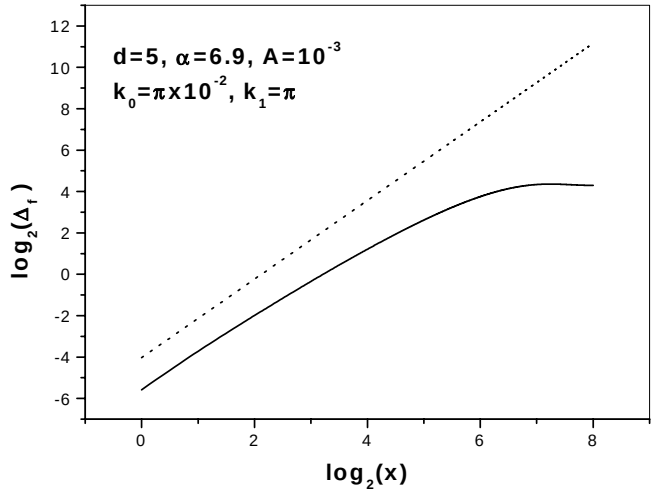

Fig. 3. The same as Figure 2, however for $d = 5$ and $\alpha = 6.9$ (close to the upper limit of the α-values) and $A = 0.001$. Note that the slope of the SF corresponding to finite hierarchy of scales surface is smaller compared to the ideal fractal surface.

Equation (17) shows that $\Delta_{(f)}(x)$ approaches $2\sigma^2$ for large x in an oscillatory manner. The leading term, namely

$$\Delta_{(f)}(x) \sim 2\sigma^2 + \frac{2A\pi^{(d-1)/2}}{k_0^{\alpha-d}} \times \left(\frac{2}{k_0 x}\right)^{(d+1)/2} \cos\left[k_0 x - \frac{\pi}{4}(d+1)\right] \quad (18)$$

shows that the amplitude of the oscillations decrease with increasing the dimension of the space in which $f(\boldsymbol{x})$ is embedded.

We conclude by defining three parameters which characterize the SF, respectively the second order statistics of the field $f(\boldsymbol{x})$ qualitatively. The first two, called cross-over distances, serve to separate more accurately the three asymptotic regimes of the SF. Following a definition suggested by Thieler [10], we obtain the first cross-over distance by equating the leading terms of (10) and (14)

$$x_{(\mathrm{co1})} = \left[\frac{d\,\Gamma(d/2)\Gamma\left((d+4-\alpha)/2\right)}{(\alpha-d)\Gamma(\alpha/2)\left(1-\delta^{d+2-\alpha}\right)}\right]^{1/(d+2-\alpha)} \frac{2}{k_1}, \quad (19)$$

where $\delta = k_0/k_1$ is introduced. The second cross-over distance is derived by equating the leading terms of (14) and (17)

$$x_{(\mathrm{co2})} = \left[\frac{\Gamma(\alpha/2)\left(1-\delta^{\alpha-d}\right)}{\Gamma(d/2)\Gamma\left((d+2-d)/2\right)}\right]^{1/(\alpha-d)} \frac{2}{k_0}\,. \quad (20)$$

The third parameter – the correlation length $l_{(\mathrm{corr})}$ – characterize distances for which $\Delta_{(f)}(\alpha, x) \approx 2\sigma^2$, or alternatively the autocovariance function of $f(\boldsymbol{x})$ is small. Requiring the second term in (18) to be small compared to the first we obtain:

$$l_{(\mathrm{corr})} = \left[\frac{(\alpha-d)\Gamma(d/2)}{2(\pi)^{1/2}\left(1-\delta^{d+2-\alpha}\right)}\right]^{2/(d+1)} \frac{2}{k_0}; \quad (21)$$

Expressions (19), (20) and (21) reduce to the analogous expressions for the case $d = 1$, given in [1,2].

4 Conclusions

We have derived an exact expression for the structure function (SF) of a random surface generated by power-law power spectra defined for every wavenumber k, and have shown that such a surface is exactly self-affine in statistical sense (ideal fractal surfaces). Next we have studied physically more realistic case of power-law spectra defined over finite spectral interval, equation (9). For them we have also computed the SF and identified three different asymptotic regimes. Systematic discrepancies of the scaling behaviour compared with the ideal fractals have been found and understood as finite-size effects. The latter reveals an intrinsic drawback of the scaling/fractal analysis, see also [1,2].

The importance of the second class of random fields is seen from the applications they find in dimensions $d = 1$ and $d = 2$. In $d = 2$, the approximate self-affine surfaces were found adequate models for metal deposits [11], ion-beam-modified Cr coatings [12] and cultivated soil roughness [13]. In $d = 1$, finite domain power-law spectra were employed to characterize experimental time series generated as stress difference between two spatial locations in a granular flow of sand in a hopper [14]. Latter they were used as building blocks to construct more elaborated multi-segmented models of computer simulated rough profiles [15,16]. Multi-segmented spectral models of the same kind describe also the two-point statistics of time series generated by low-dimensional chaotic dynamics systems [2,17].

The method used to build the above models has the following advantages over the more familiar and simple scaling or fractal methods: It describes the full two-point statistics of the phenomena, provides more accurate estimation of all specific parameters (not just the scaling exponents), incorporates the finite site effects explicitly and avoids dealing with singular functions. Applications of this method for $d \geq 3$, can easily be envisioned in developed turbulence and higher dimensional chaotic systems.

Appendix

In this appendix we enlist the integral representation and the asymptotic expansion used in Section 3 to obtain the expressions for the field's structure functions.

First we have

$${}_1F_2\left(\frac{\mu-\alpha}{2}; \frac{\mu+2-\alpha}{2}, \frac{\mu}{2}; -\frac{z^2}{4}\right) = 1 + (\alpha-\mu)z^{\alpha-\mu}\int_0^z \left(1 - {}_0F_1\left(\frac{\mu}{2}; -\frac{x^2}{4}\right)\right) x^{\mu-\alpha-1}\mathrm{d}x \quad (22)$$

which as it can be verified in a straightforward manner is valid for $\alpha < \mu + 2$. With the further restriction $\alpha > \mu$, it is easy to develop an asymptotic expansion of ${}_1F_2$ from (22) for large z. For this purpose we first extend the upper limit of integration to ∞ and subtract an integral from the same integrand evaluated within the limits (z, ∞). The first integral (from zero) can be computed in a closed form, *cf.* with the expression pertaining to the ideal fractal fields, Section 2. The second integral is integrated repeatedly by parts leading to an asymptotic series in inverse powers of z. Combining both terms into (22), the desired asymptotic form of ${}_1F_2$ reads:

$$
\begin{aligned}
&{}_1F_2\left(\frac{\mu-\alpha}{2}; \frac{\mu+2-\alpha}{2}, \frac{\mu}{2}; -\frac{z^2}{4}\right) \approx \\
&\Gamma\left(\frac{\mu}{2}\right) \frac{\Gamma\left((\mu-\alpha)/2+1\right)}{\Gamma(\alpha/2)} \left(\frac{z}{2}\right)^{\alpha-\mu} \\
&-\left(\frac{\alpha-\mu}{\mu}\right) {}_0F_1\left(\frac{\mu+2}{2}; -\frac{z^2}{4}\right) Y_0(z) \\
&+\left(\frac{\alpha-\mu}{z}\right) {}_0F_1\left(\frac{\mu}{2}; -\frac{z^2}{4}\right) Y_1(z) \qquad (23)
\end{aligned}
$$

where $Y_p(z)$, $p = 1, 2$, are the asymptotic series given by (16).

References

1. O.I. Yordanov, N.I. Nickolaev, Phys. Rev. E **49**, R2517 (1994)
2. O.I. Yordanov, N.I. Nickolaev, Physica D **101**, 116 (1997)
3. M.A. Priestley, *Spectral Analysis and Time Series* (Academic Press, London, 1981)
4. M.V. Berry, J. Phys. A **12**, 781 (1979)
5. M. Abramowitz, I.A. Stegun, *Handbook of Mathematical Functions* (Dover, New York, 1970)
6. L.J. Slater, *Generalized Hypergeometric Functions* (Cambridge University Press, London, 1966)
7. S. Orey, Z. Wahrsch'theorie verw. Geb. **15**, 249 (1970); K.J. Falconer, *The Geometry of Fractal Sets* (Cambridge University Press, Cambridge, 1985)
8. R.S. Sayles, T.R. Thomas, Nature **271**, 431 (1978); M.V. Berry, J.H. Hannay, Nature **273**, 573 (1978)
9. N.P. Greis, H.S. Greenside, Phys. Rev. A **44**, 2324 (1991)
10. J. Theiler, Phys. Lett. A **155**, 480 (1991)
11. O.I. Yordanov, K. Ivanova, Surf. Sci. **331-333**, 1043 (1995)
12. M. Holzwarth, M. Wiing, D.S. Simeonova, S. Tzanev, K.J. Snowdon, O.I. Yordanov, Surf. Sci. **331-333**, 1093 (1995)
13. O.I. Yordanov, A. Guissard, Physica A **238**, 49 (1997)
14. R. Kant, Phys. Rev. E **53**, 5749 (1996)
15. I.S. Atanasov, O.I. Yordanov, *Proc. NATO Adv. Res. Workshop on "Nano-crystalline and thin film magnetic oxides", 1998, Sozopol, Bulgaria*, edited by M. Ausloos, I. Nedkov (Kluwer Academic Publishers, 1998), pp. 293–300
16. L.A. Vulkova, I.A. Atanasov, O.I. Yordanov, Vacuum **58**, 158 (2000)
17. E.S. Dimitrova, O.I. Yordanov, Int. J. Bifurc. Chaos **11**, 2675 (2001)